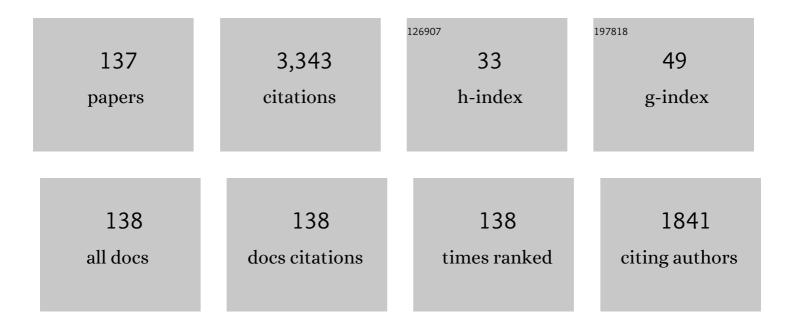
Lorenzo Frassinetti

List of Publications by Year in descending order

Source: https://exaly.com/author-pdf/6963161/publications.pdf Version: 2024-02-01



#	Article	IF	CITATIONS
1	Impact of nitrogen seeding on confinement and power load control of a high-triangularity JET ELMy H-mode plasma with a metal wall. Nuclear Fusion, 2013, 53, 113025.	3.5	118
2	A Key to Improved Ion Core Confinement in the JET Tokamak: Ion Stiffness Mitigation due to Combined Plasma Rotation and Low Magnetic Shear. Physical Review Letters, 2011, 107, 135004.	7.8	106
3	Overview of quasi-single helicity experiments in reversed field pinches. Nuclear Fusion, 2003, 43, 1855-1862.	3.5	102
4	Spatial resolution of the JET Thomson scattering system. Review of Scientific Instruments, 2012, 83, 013506.	1.3	90
5	ELM-induced transient tungsten melting in the JET divertor. Nuclear Fusion, 2015, 55, 023010.	3.5	83
6	Pedestal confinement and stability in JET-ILW ELMy H-modes. Nuclear Fusion, 2015, 55, 113031.	3.5	82
7	Improved confinement in JET highβplasmas with an ITER-like wall. Nuclear Fusion, 2015, 55, 053031.	3.5	79
8	H-mode pedestal scaling in DIII-D, ASDEX Upgrade, and JET. Physics of Plasmas, 2011, 18, 056120.	1.9	76
9	The effect of a metal wall on confinement in JET and ASDEX Upgrade. Plasma Physics and Controlled Fusion, 2013, 55, 124043.	2.1	70
10	The role of the density profile in the ASDEX-Upgrade pedestal structure. Plasma Physics and Controlled Fusion, 2017, 59, 014017.	2.1	69
11	Progress at JET in integrating ITER-relevant core and edge plasmas within the constraints of an ITER-like wall. Plasma Physics and Controlled Fusion, 2015, 57, 035004.	2.1	64
12	First scenario development with the JET new ITER-like wall. Nuclear Fusion, 2014, 54, 013011.	3.5	59
13	Integration of a radiative divertor for heat load control into JET high triangularity ELMy H-mode plasmas. Nuclear Fusion, 2012, 52, 063022.	3.5	58
14	First operation with the JET International Thermonuclear Experimental Reactor-like wall. Physics of Plasmas, 2013, 20, .	1.9	56
15	ELM induced tungsten melting and its impact on tokamak operation. Journal of Nuclear Materials, 2015, 463, 78-84.	2.7	53
16	MHD and gyro-kinetic stability of JET pedestals. Nuclear Fusion, 2013, 53, 123012.	3.5	52
17	Overview of the TCV tokamak program: scientific progress and facility upgrades. Nuclear Fusion, 2017, 57, 102011.	3.5	52
18	Global and pedestal confinement in JET with a Be/W metallic wall. Nuclear Fusion, 2014, 54, 043001.	3.5	47

#	Article	IF	CITATIONS
19	Scenario development for D–T operation at JET. Nuclear Fusion, 2019, 59, 076037.	3.5	46
20	A new paradigm for RFP magnetic self-organization: results and challenges. Plasma Physics and Controlled Fusion, 2007, 49, A177-A193.	2.1	45
21	Predictive multi-channel flux-driven modelling to optimise ICRH tungsten control and fusion performance in JET. Nuclear Fusion, 2020, 60, 066029.	3.5	45
22	Pedestal width and ELM size identity studies in JET and DIII-D; implications for ITER. Plasma Physics and Controlled Fusion, 2009, 51, 124051.	2.1	44
23	The H-mode pedestal structure and its role on confinement in JET with a carbon and metal wall. Nuclear Fusion, 2015, 55, 013019.	3.5	43
24	Role of the pedestal position on the pedestal performance in AUG, JET-ILW and TCV and implications for ITER. Nuclear Fusion, 2019, 59, 076038.	3.5	43
25	Physics research on the TCV tokamak facility: from conventional to alternative scenarios and beyond. Nuclear Fusion, 2019, 59, 112023.	3.5	43
26	Integrated modelling of H-mode pedestal and confinement in JET-ILW. Plasma Physics and Controlled Fusion, 2018, 60, 014042.	2.1	40
27	Mitigation of type-I ELMs with <i>n</i> = 2 fields on JET with ITER-like wall. Nuclear Fusion, 2013, 53, 073036.	3.5	39
28	Effect of the relative shift between the electron density and temperature pedestal position on the pedestal stability in JET-ILW and comparison with JET-C. Nuclear Fusion, 2018, 58, 056010.	3.5	38
29	Overview of physics studies on ASDEX Upgrade. Nuclear Fusion, 2019, 59, 112014.	3.5	38
30	Contrasting H-mode behaviour with deuterium fuelling and nitrogen seeding in the all-carbon and metallic versions of JET. Nuclear Fusion, 2014, 54, 073016.	3.5	37
31	Physics of Plasmas, 2015, 22, 056115.	1.9	37
32	Global performance enhancements via pedestal optimisation on ASDEX Upgrade. Plasma Physics and Controlled Fusion, 2017, 59, 025010.	2.1	36
33	Impact of wall materials and seeding gases on the pedestal and on core plasma performance. Nuclear Materials and Energy, 2017, 12, 18-27.	1.3	36
34	Spontaneous quasi single helicity regimes in EXTRAP T2R reversed-field pinch. Physics of Plasmas, 2007, 14, 112510.	1.9	35
35	Dependence on plasma shape and plasma fueling for small edge-localized mode regimes in TCV and ASDEX Upgrade. Nuclear Fusion, 2019, 59, 086020.	3.5	34
36	Microtearing modes as the source of magnetic fluctuations in the JET pedestal. Nuclear Fusion, 2021, 61, 036015.	3.5	32

#	Article	IF	CITATIONS
37	Tomographic imaging of resistive mode dynamics in the Madison Symmetric Torus reversed-field pinch. Physics of Plasmas, 2006, 13, 012510.	1.9	30
38	Resonant magnetic perturbation effect on tearing mode dynamics. Nuclear Fusion, 2010, 50, 035005.	3.5	30
39	Studies of the pedestal structure and inter-ELM pedestal evolution in JET with the ITER-like wall. Nuclear Fusion, 2017, 57, 116012.	3.5	30
40	Overview of the TCV tokamak experimental programme. Nuclear Fusion, 2022, 62, 042018.	3.5	30
41	Pedestal study across a deuterium fuelling scan for high <i>δ</i> ELMy H-mode plasmas on JET with the carbon wall. Nuclear Fusion, 2013, 53, 083028.	3.5	29
42	Plasma density and temperature evolution following the H-mode transition at JET and implications for ITER. Nuclear Fusion, 2013, 53, 083031.	3.5	27
43	Pedestal structure, stability and scalings in JET-ILW: the EUROfusion JET-ILW pedestal database. Nuclear Fusion, 2021, 61, 016001.	3.5	27
44	Electron temperature profiles in RFX-mod. Plasma Physics and Controlled Fusion, 2008, 50, 035013.	2.1	26
45	Numerical evaluation of heat flux and surface temperature on a misaligned JET divertor W lamella during ELMs. Nuclear Fusion, 2014, 54, 123011.	3.5	26
46	Dimensionless scalings of confinement, heat transport and pedestal stability in JET-ILW and comparison with JET-C. Plasma Physics and Controlled Fusion, 2017, 59, 014014.	2.1	26
47	Self-consistent pedestal prediction for JET-ILW in preparation of the DT campaign. Physics of Plasmas, 2019, 26, .	1.9	26
48	Analysis and modelling of the magnetic and plasma profiles during PPCD experiments in RFX. Nuclear Fusion, 2003, 43, 1057-1065.	3.5	25
49	Comparison of hybrid and baseline ELMy H-mode confinement in JET with the carbon wall. Nuclear Fusion, 2013, 53, 013001.	3.5	25
50	Recent progress in the quantitative validation of JOREK simulations of ELMs in JET. Nuclear Fusion, 2017, 57, 076006.	3.5	25
51	Isotope dependence of energy, momentum and particle confinement in tokamaks. Journal of Plasma Physics, 2020, 86, .	2.1	25
52	First principle-based multi-channel integrated modelling in support of the designÂof the Divertor Tokamak Test facility. Nuclear Fusion, 2021, 61, 116068.	3.5	25
53	Improved Particle Confinement in Transition from Multiple-Helicity to Quasi-Single-Helicity Regimes of a Reversed-Field Pinch. Physical Review Letters, 2006, 97, 175001.	7.8	24
54	Impact of divertor geometry on H-mode confinement in the JET metallic wall. Nuclear Fusion, 2017, 57, 086025.	3.5	24

#	Article	IF	CITATIONS
55	Role of the separatrix density in the pedestal performance in deuterium low triangularity JET-ILW plasmas and comparison with JET-C. Nuclear Fusion, 2021, 61, 126054.	3.5	24
56	Overview of progress in European medium sized tokamaks towards an integrated plasma-edge/wall solution ^a . Nuclear Fusion, 2017, 57, 102014.	3.5	23
57	Ion heat transport studies in JET. Plasma Physics and Controlled Fusion, 2011, 53, 124033.	2.1	22
58	Global and pedestal confinement and pedestal structure in dimensionless collisionality scans of low-triangularity H-mode plasmas in JET-ILW. Nuclear Fusion, 2017, 57, 016012.	3.5	22
59	Non-linear MHD simulations of ELMs in JET and quantitative comparisons to experiments. Plasma Physics and Controlled Fusion, 2016, 58, 014026.	2.1	20
60	The role of ETG modes in JET–ILW pedestals with varying levels of power and fuelling. Nuclear Fusion, 2022, 62, 086028.	3.5	20
61	The role of carbon and nitrogen on the H-mode confinement in ASDEX Upgrade with a metal wall. Nuclear Fusion, 2016, 56, 056014.	3.5	19
62	Impact of toroidal and poloidal mode spectra on the control of non-axisymmetric fields in tokamaks. Physics of Plasmas, 2017, 24, .	1.9	19
63	Pedestal structure and energy confinement studies on TCV. Plasma Physics and Controlled Fusion, 2019, 61, 014002.	2.1	19
64	Tearing mode velocity braking due to resonant magnetic perturbations. Nuclear Fusion, 2012, 52, 103014.	3.5	18
65	Investigation of the influence of divertor recycling on global plasma confinement in JET ITER-like wall. Journal of Nuclear Materials, 2015, 463, 450-454.	2.7	18
66	Overview of the RFX-mod contribution to the international Fusion Science Program. Nuclear Fusion, 2015, 55, 104012.	3.5	18
67	Quasi-single helicity state at shallow reversal in TPE-RX reversed-field pinch experiment. Physics of Plasmas, 2005, 12, 112501.	1.9	17
68	Overview of the RFX-mod fusion science programme. Nuclear Fusion, 2013, 53, 104018.	3.5	17
69	Analysis of ELM stability with extended MHD models in JET, JT-60U and future JT-60SA tokamak plasmas. Plasma Physics and Controlled Fusion, 2018, 60, 014032.	2.1	17
70	Resistive wall mode feedback control in EXTRAP T2R with improved steady-state error and transient response. Physics of Plasmas, 2007, 14, 102505.	1.9	16
71	Error field assessment from driven rotation of stable external kinks at EXTRAP-T2R reversed field pinch. Nuclear Fusion, 2013, 53, 043018.	3.5	16
72	Effect of nitrogen seeding on the energy losses and on the time scales of the electron temperature and density collapse of type-I ELMs in JET with the ITER-like wall. Nuclear Fusion, 2015, 55, 023007.	3.5	16

#	Article	IF	CITATIONS
73	Insights into typeâ€l edge localized modes and edge localized mode control from JOREK nonâ€linear magnetoâ€hydrodynamic simulations. Contributions To Plasma Physics, 2018, 58, 518-528.	1.1	16
74	Heat diffusivity model and temperature simulations in RFX-mod. Nuclear Fusion, 2008, 48, 045007.	3.5	15
75	Braking due to non-resonant magnetic perturbations and comparison with neoclassical toroidal viscosity torque in EXTRAP T2R. Nuclear Fusion, 2015, 55, 112003.	3.5	15
76	Development of the Q  =  10 scenario for ITER on ASDEX Upgrade (AUG). Nuclear Fusion, 201	6, 5 6, 106	0075
77	Recent progress in L–H transition studies at JET: tritium, helium, hydrogen and deuterium. Nuclear Fusion, 2022, 62, 076026.	3.5	15
78	Overview of results in the MST reversed field pinch experiment. Nuclear Fusion, 2005, 45, S276-S282.	3.5	14
79	Reduced intermittency in the magnetic turbulence of reversed field pinch plasmas. Physics of Plasmas, 2005, 12, 030701.	1.9	14
80	Edge Thomson scattering diagnostic on COMPASS tokamak: Installation, calibration, operation, improvements. Review of Scientific Instruments, 2014, 85, 11E431.	1.3	14
81	Thermal analysis of an exposed tungsten edge in the JET divertor. Journal of Nuclear Materials, 2015, 463, 415-419.	2.7	14
82	Pedestal evolution physics in low triangularity JET tokamak discharges with ITER-like wall. Nuclear Fusion, 2018, 58, 016021.	3.5	14
83	Experiments and modelling of active quasi-single helicity regime generation in a reversed field pinch. Nuclear Fusion, 2009, 49, 075019.	3.5	13
84	Implementation of advanced feedback control algorithms for controlled resonant magnetic perturbation physics studies on EXTRAP T2R. Nuclear Fusion, 2011, 51, 063018.	3.5	13
85	The tearing mode locking–unlocking mechanism to an external resonant field in EXTRAP T2R. Plasma Physics and Controlled Fusion, 2014, 56, 104001.	2.1	13
86	Numerical analysis of ELM stability with rotation and ion diamagnetic drift effects in JET. Nuclear Fusion, 2017, 57, 126001.	3.5	11
87	Long-lived coupled peeling ballooning modes preceding ELMs on JET. Nuclear Fusion, 2019, 59, 056004.	3.5	11
88	Isotope dependence of the type I ELMy H-mode pedestal in JET-ILW hydrogen and deuterium plasmas. Nuclear Fusion, 2021, 61, 046015.	3.5	11
89	DIII-D research advancing the physics basis for optimizing the tokamak approach to fusion energy. Nuclear Fusion, 2022, 62, 042024.	3.5	11
90	Experimental study on the role of the target electron temperature as a key parameter linking recycling to plasma performance in JET-ILW*. Nuclear Fusion, 2022, 62, 066030.	3.5	11

#	Article	IF	CITATIONS
91	An empirical scaling law for improved confinement in reversed-field pinch plasmas. Nuclear Fusion, 2005, 45, 138-142.	3.5	10
92	Cold pulse propagation in a reversed-field pinch. Nuclear Fusion, 2007, 47, 135-145.	3.5	10
93	Implementation of model predictive control for resistive wall mode stabilization on EXTRAP T2R. Plasma Physics and Controlled Fusion, 2015, 57, 104005.	2.1	10
94	ELM behavior in ASDEX Upgrade with and without nitrogen seeding. Nuclear Fusion, 2017, 57, 022004.	3.5	10
95	The dependence of exhaust power components on edge gradients in JET-C and JET-ILW H-mode plasmas. Plasma Physics and Controlled Fusion, 2020, 62, 055010.	2.1	10
96	The dependence of confinement on the isotope mass in the core and the edge of AUG and JET-ILW H-mode plasmas. Nuclear Fusion, 2022, 62, 026014.	3.5	10
97	ELM control at the L → H transition by means of pellet pacing in the ASDEX Upgrade and JET all-metal-wall tokamaks. Plasma Physics and Controlled Fusion, 2015, 57, 045011.	2.1	9
98	Dependence of Perpendicular Viscosity on Magnetic Fluctuations in a Stochastic Topology. Physical Review Letters, 2018, 120, 225002.	7.8	9
99	Change in the pedestal stability between JET-C and JET-ILW low triangularity peeling-ballooning limited plasmas. Nuclear Fusion, 2021, 61, 026008.	3.5	9
100	Performance improvement conditions and their physical origin in the pulsed poloidal current drive regime of the reversed-field pinch device TPE-RX. Physics of Plasmas, 2004, 11, 5229-5238.	1.9	8
101	Recent improvements in confinement and beta in the MST reversed-field pinch. Nuclear Fusion, 2007, 47, L17-L20.	3.5	8
102	Effect of poloidal phasing on ion cyclotron resonance heating power absorption. Nuclear Fusion, 2019, 59, 076022.	3.5	8
103	Turbulence and particle confinement in a reversed-field pinch plasma. Plasma Physics and Controlled Fusion, 2007, 49, 199-209.	2.1	7
104	Heat transport in the quasi-single-helicity islands of EXTRAP T2R. Physics of Plasmas, 2009, 16, 032503.	1.9	7
105	Edge profile analysis of Joint European Torus (JET) Thomson scattering data: Quantifying the systematic error due to edge localised mode synchronisation. Review of Scientific Instruments, 2016, 87, 013507.	1.3	7
106	Hysteresis in the tearing mode locking/unlocking due to resonant magnetic perturbations in EXTRAP T2R. Plasma Physics and Controlled Fusion, 2015, 57, 104008.	2.1	7
107	A survey of pedestal magnetic fluctuations using gyrokinetics and a global reduced model for microtearing stability. Physics of Plasmas, 2022, 29, .	1.9	7
108	Density pump-out compensation during type-I edge localized mode control experiments withn= 1 perturbation fields on JET. Plasma Physics and Controlled Fusion, 2011, 53, 085009.	2.1	6

#	Article	IF	CITATIONS
109	A first attempt at few coils and low-coverage resistive wall mode stabilization of EXTRAP T2R. Plasma Physics and Controlled Fusion, 2012, 54, 094005.	2.1	6
110	Impact of the JET ITER-like wall on H-mode plasma fueling. Nuclear Fusion, 2017, 57, 066024.	3.5	6
111	Contribution to the multi-machine pedestal scaling from the COMPASS tokamak. Nuclear Fusion, 2017, 57, 056041.	3.5	6
112	Control of the hydrogen:deuterium isotope mixture using pellets in JET. Nuclear Fusion, 2019, 59, 106047.	3.5	6
113	Towards understanding reactor relevant tokamak pedestals. Nuclear Fusion, O, , .	3.5	6
114	Operating Conditions to Achieve High Performance in PPCD in a Reversed-Field Pinch Plasma. Journal of the Physical Society of Japan, 2003, 72, 3297-3298.	1.6	6
115	Perturbative transport studies in the reversed-field pinch. Nuclear Fusion, 2005, 45, 1342-1349.	3.5	5
116	Role of locked mode in the effectiveness of pulsed poloidal current drive regime in the reversed-field pinch. Physics of Plasmas, 2005, 12, 100703.	1.9	5
117	Heat transport modelling in EXTRAP T2R. Nuclear Fusion, 2009, 49, 025002.	3.5	5
118	Measurement of Fast Magnetic Fluctuations in Edge Region of TPE-RX Reversed-Field Pinch Plasma. Japanese Journal of Applied Physics, 2007, 46, 6831-6833.	1.5	4
119	Transport asymmetry and release mechanisms of metal dust in the reversed-field pinch configuration. Plasma Physics and Controlled Fusion, 2014, 56, 035014.	2.1	4
120	Tearing mode dynamics and locking in the presence of external magnetic perturbations. Physics of Plasmas, 2016, 23, .	1.9	4
121	Improved model predictive control of resistive wall modes by error field estimator in EXTRAP T2R. Plasma Physics and Controlled Fusion, 2016, 58, 124002.	2.1	4
122	Inter-ELM evolution of the edge current density in JET-ILW type I ELMy H-mode plasmas. Plasma Physics and Controlled Fusion, 2018, 60, 085003.	2.1	4
123	Impact of the new TCV baffled divertor upgrade on pedestal structure and performance. Nuclear Materials and Energy, 2021, 26, 100933.	1.3	4
124	Toroidally localized soft x-ray expulsion at the termination of the improved confinement regime in the TPE-RX reversed-field pinch experiment. Physics of Plasmas, 2006, 13, 042502.	1.9	3
125	Metal impurity fluxes and plasma-surface interactions in EXTRAP T2R. Journal of Physics: Conference Series, 2008, 100, 062030.	0.4	3
126	A method for the estimate of the wall diffusion for non-axisymmetric fields using rotating external fields. Plasma Physics and Controlled Fusion, 2013, 55, 084001.	2.1	3

#	ARTICLE	IF	CITATIONS
127	Intra-ELM tungsten sputtering in JET ITER-like wall: analytical studies of Be impurity and ELM type influence. Physica Scripta, 2017, T170, 014065.	2.5	3
128	Frequency Dependence of Fast Magnetic Fluctuations in TPE-RX Reversed-Field Pinch Plasma. Plasma and Fusion Research, 2008, 3, 060-060.	0.7	3
129	Soft X-ray pulses in the reversed-field pinch. IEEE Transactions on Plasma Science, 2005, 33, 462-463.	1.3	2
130	Studies of the non-axisymmetric plasma boundary displacement in JET in presence of externally applied magnetic field. Plasma Physics and Controlled Fusion, 2015, 57, 104003.	2.1	2
131	Design and operation of fast model predictive controller for stabilization of magnetohydrodynamic modes in a fusion device. , 2015, , .		2
132	Local measurement of error field using naturally rotating tearing mode dynamics in EXTRAP T2R. Plasma Physics and Controlled Fusion, 2016, 58, 124001.	2.1	2
133	Gray-box modeling of resistive wall modes with vacuum-plasma separation and optimal control design for EXTRAP T2R. Fusion Engineering and Design, 2017, 121, 245-255.	1.9	2
134	Enabling adaptive pedestals in predictive transport simulations using neural networks. Nuclear Fusion, 2022, 62, 096006.	3.5	2
135	ELM size analysis in JET hybrid plasmas. Nuclear Fusion, 2011, 51, 112001.	3.5	1
136	The magnitude of sawtooth crash events in multiple and quasi-single helicity states in a reversed-field-pinch plasma. Physics of Plasmas, 2005, 12, 082507.	1.9	0
137	Understanding JET-C quiescent phases with edge harmonic magnetohydrodynamic activity and comparison with behaviour under ITER-like wall conditioning. Plasma Physics and Controlled Fusion, o	2.1	Ο